

Tyrosine-based Membrane Protein Sorting Signals Are Differentially Interpreted by Polarized Madin-Darby Canine Kidney and LLC-PK₁ Epithelial Cells*

(Received for publication, May 8, 1998, and in revised form, July 22, 1998)

Denise L. Roush^{‡§}, Cara J. Gottardi^{‡¶}, Hussein Y. Naim^{||}, Michael G. Roth^{||},
and Michael J. Caplan^{‡**}

From the [‡]Department of Cellular and Molecular Physiology, Yale University School of Medicine, New Haven, Connecticut 06510 and the ^{||}Department of Biochemistry, University of Texas Southwestern Medical Center, Dallas, Texas 75235

Tyrosine-dependent sequence motifs are implicated in sorting membrane proteins to the basolateral domain of Madin-Darby canine kidney (MDCK) cells. We find that these motifs are interpreted differentially in various polarized epithelial cell types. The H,K-ATPase β subunit, which contains a tyrosine-based motif in its cytoplasmic tail, was expressed in MDCK and LLC-PK₁ cells. This protein was restricted to the basolateral membrane in MDCK cells, but was localized to the apical membrane in LLC-PK₁ cells. Similarly, HA-Y543, a construct in which a tyrosine-based motif was introduced into the cytoplasmic tail of influenza hemagglutinin, was sorted to the basolateral membrane of MDCK cells and retained at the apical membrane of LLC-PK₁ cells. A chimera in which the cytoplasmic tail of the H,K-ATPase β subunit protein was replaced with the analogous region of the Na,K-ATPase β subunit polypeptide was localized to both surface domains of MDCK cells. Mutation of tyrosine-20 of the H,K-ATPase β subunit cytoplasmic sequence to an alanine was sufficient to disrupt basolateral localization of this polypeptide. In contrast, these constructs all remain localized to the apical membrane in LLC-PK₁ cells. The FcR2 protein bears a dileucine motif and is found at the basolateral membrane of both MDCK and LLC-PK₁ cells. These results demonstrate that polarized epithelia are able to discriminate between different classes of specifically defined membrane protein sorting signals.

modeling of the plasma membrane. Information specifying sorting behavior must, therefore, be encoded within the structure of each individual plasma membrane protein. Furthermore, these signals must be correctly recognized and interpreted by sorting machinery to dictate proper targeting.

A number of sequence motifs, which mediate the sorting of membrane proteins to various polarized domains, have recently been described. The transmembrane (3, 4)¹ and ectodomains (5–7) of several polypeptides have been implicated in mediating delivery to the apical domain. Several classes of sequences have been found to direct specific sorting to the basolateral domain in the polarized kidney epithelial cell line, MDCK.² pIGR (8) contains a unique basolateral sorting sequence that does not appear to be found in other basolateral polypeptides. A second class of basolateral sorting motif, which encompasses a critical tyrosine residue, has been found in a wide variety of membrane proteins (9–13). These motifs appear to take the form YXX-aliphatic amino acid (14). Similar sequences have also been shown to mediate internalization into endosomes via clathrin-coated pits (15, 16). A representative of such an internalization signal is the YXRF sequence found in the cytoplasmic tail of the transferrin receptor (17). In addition, Brewer and Roth found that a single point mutation introducing a tyrosine-dependent endocytosis sequence (HA-Y543) into the cytoplasmic tail of the influenza hemagglutinin (HA) protein was sufficient to override the apical sorting signal previously demonstrated in that protein. HA-Y543 is sorted to the basolateral domain of MDCK cells (12). Tyrosine-independent di-leucine endocytosis sequence motifs constitute yet a third class of basolateral sorting signal (18–20).

We have begun to identify the protein domains of a heterodimeric ion pump, the gastric H,K-ATPase, which are responsible for its localization in polarized epithelial cells. We have previously demonstrated that the H,K-ATPase β subunit is sorted both to the apical domain and to a subapical population of endosomes in an epithelial cell line derived from the mammalian kidney, LLC-PK₁ (21). Analysis of the N-terminal cytoplasmic domain of the H,K-ATPase β subunit revealed the presence of a putative tyrosine-based motif (FRHY). Because the H,K-ATPase β subunit is a type II membrane protein, this motif is presented in reverse orientation to the YXX-aliphatic amino acid sequence discussed above. However, reversing the orientation of similar tyrosine-based motifs in the transferrin

Polarized epithelial cells serve as barriers between compositionally dissimilar environments. Their plasma membranes are divided into apical and basolateral domains, which are separated by tight junctions. These domains are composed of distinct sets of proteins and lipids, allowing them to serve diverse physiological functions (1, 2). Newly synthesized membrane proteins are delivered to the sites of their ultimate functional residence and retained there throughout continuous re-

* This work was supported by National Institutes of Health Grants GM-42136 and DK-17433 (to M. J. C.). The costs of publication of this article were defrayed in part by the payment of page charges. This article must therefore be hereby marked "advertisement" in accordance with 18 U.S.C. Section 1734 solely to indicate this fact.

§ Present address: Laboratory of Cellular and Developmental Biology, NIDDK, National Institutes of Health, 9000 Rockville Pike, Bethesda, MD 20852.

¶ Present address: Dept. of Cell Biology, Memorial Sloan Kettering Cancer Center, 1275 York Ave., New York, NY 10021.

** To whom correspondence should be addressed: Dept. of Cellular and Molecular Physiology, Yale University School of Medicine, 333 Cedar St., New Haven, CT 06510. Tel.: 203-785-7316; Fax: 203-785-4951.

¹ L. Dunbar and M. Caplan, manuscript in preparation.

² The abbreviations used are: MDCK, Madin-Darby canine kidney; HA hemagglutinin; LDL, low density lipoprotein; PBS, phosphate-buffered saline; BSA, bovine serum albumin; Ab, antibody; PAGE, polyacrylamide gel electrophoresis; DMEM, Dulbecco's modified Eagle's medium.

and LDL receptors has been shown to reduce, but not to abolish, their competence to mediate internalization (22). We have also demonstrated that this motif mediates internalization of the H,K-ATPase from the surfaces of gastric parietal cells *in vivo* (51). Because tyrosine-dependent motifs have been shown to direct basolateral sorting in MDCK cells, we wondered whether the apical localization of this protein in LLC-PK₁ cells was indicative of a cell-type specific difference in the interpretation of this motif.

It has previously been demonstrated that the H,K-ATPase β subunit is able to leave the endoplasmic reticulum without the requirement for assembly with its corresponding α subunit (23). The Na,K-ATPase β subunit cannot leave the endoplasmic reticulum before assembly with the Na,K-ATPase α subunit. Although the Na,K-ATPase β subunit is approximately 35% identical to the H,K-ATPase β subunit, it does not contain a comparable tyrosine-dependent motif. We have taken advantage of these attributes in creating constructs designed to determine whether the tyrosine-based motif present in the H,K-ATPase β subunit is responsible for the different sorting behavior of this polypeptide in MDCK and LLC-PK₁ cells. Furthermore, the distribution of the FcR2-B2 polypeptide, which contains a di-leucine motif (18, 19, 24), was examined to determine whether other classes of sorting signals are differentially interpreted by these two polarized cell types.

EXPERIMENTAL PROCEDURES

Cell Culture and Stable Transfection

MDCK cells (gift of K. Matlin, Massachusetts General Hospital, Boston, MA) were maintained in minimal essential medium with Earle's salts (Life Technologies, Inc.), 10% fetal calf serum (Sigma), 50 units/ml penicillin, 50 mg/ml streptomycin, and 2 mM L-glutamine. LLC-PK₁ (gift of K. Amsler, Robert Wood Johnson Medical School, Piscataway, NJ) cells were maintained in minimal essential medium alpha medium (Life Technologies, Inc.), supplemented as described for the MDCK cells. All cells were grown in a humidified incubator at 37 °C and 5% CO₂ atmosphere. The rabbit gastric H,K-ATPase β cDNA was kindly provided by M. Reuben and G. Sachs (University of California, Los Angeles, CA) (25). The rat Na,K-ATPase β 1 cDNA was kindly provided by E. Benz (Johns Hopkins University). FcR2-B2 was kindly provided by I. Mellman (Yale University, New Haven, CT). All cDNAs, including the wild type HA and the HA-Y543 mutant, were subcloned into the cytomegalovirus promoter-based mammalian expression vector pCB6 (12) and transfected into MDCK and LLC-PK₁ cells as described previously (21). Transfected MDCK and LLC-PK₁ colonies were selected in 0.9 or 1.4 mg/ml G418 (Life Technologies, Inc.), respectively, and screened by immunofluorescence and Western blot. LLC-PK₁ cells expressing HA-Y543 were sorted by means of a fluorescence-activated cell sorter to generate high and low expressing cell lines. In this procedure, cells were trypsinized and suspended in media containing fluorescein isothiocyanate-conjugated antibody directed against the anti-HA protein (gift of L. Roman, Johns Hopkins University, Baltimore, MD). Cells in the highest and lowest deciles of fluorescence above background were recovered and expanded after washing.

H,K/Na,K-ATPase β Subunit Chimera Construction

The H,K/Na,K-ATPase β subunit constructs were each generated by two separate polymerase chain reactions. Reaction I generated the amino terminus, containing the unique *Cla*I restriction enzyme site, up to the proposed mutation. Reaction II generated from the proposed mutation to a unique restriction enzyme site contained within the transmembrane domain of the H,K-ATPase β (A7II). The products from these reactions were then annealed at the overlapping mutation sites and amplified. A new restriction enzyme site, *Eag*I, was introduced into β N28H to provide an overlapping region for annealing the halves of this chimera. The introduction of this restriction site did not alter amino acid sequence. The full-length β subunit chimeras were isolated on 1.5% low melting temperature agarose gels, purified by Gene Clean (BIO 101, Vista, CA) and subcloned into H,K-ATPase β pCB6. All full-length chimeras were sequenced for fidelity. H,K-ATPase β pCB6 and Na,K-ATPase β 1 pBluescript SK+ (only reaction I, β N28H) were used as template cDNAs. Primers introducing the appropriate mutations (bold) are indicated; β N28H, 5'-GGTCCGGCCGAGAACTC3', and β H-

Y20A, 5'-GTTCCAGCAGGCGTGGCGGAA3' (35). 50- μ l reactions (2 μ M each primer, 0.1 mM template cDNA, 0.2 mM of each dATP, dTTP, dCTP, dGTP, 1 \times Vent DNA polymerase reaction buffer, 1 unit Vent polymerase (New England Biolabs, Beverly, MA) were run under the conditions indicated: β N28H; melt; 97 °C, 15 s; anneal; 40 °C, 120 s; extend; 72 °C, 90 s; 30 cycles; dGTP was replaced with a 3:1 ratio of 7-deaza-2'-dGTP to dGTP, and β H-Y20A; melt; 97 °C 15 s; anneal; 50 °C, 60 s; extend; 72 °C, 60 s; 30 cycles. These products were isolated and purified on 1.5% low melting temperature agarose gels (Bio-Rad, Hercules, CA). The gel slices were melted at 80 °C for 5 min and the appropriate halves of each chimera annealed at their internal overlapping regions. To anneal the reaction products, 50- μ l reactions containing 1:1 ratios of reaction product I to reaction product II in place of primers were run for 10 cycles according to the conditions specified: β H-Y20A; melt; 97 °C, 15 s; anneal; 37 °C, 90 s; extend; 72 °C, 30 s; 30 cycles, β N28H; melt; 97 °C, 15 s; anneal; 45 °C, 60 s; extend; 72 °C, 60 s; 30 cycles, dGTP was replaced with a 3:1 ratio of 7-deaza-2'-dGTP to dGTP. Annealed front to back chimeras were then amplified by the addition of 2 μ M of the outermost (unique restriction enzyme containing) primers and continuation of the reaction for an additional 20 cycles.

Immunofluorescence

Surface—Cells were plated on 0.4 μ M Transwell polycarbonate filters (Corning Costar Inc., Cambridge, MA) and allowed to establish confluency for 5–7 days. Filters were moved to 4 °C, rinsed with PBS + 0.1% BSA and incubated in HK β primary Ab (monoclonal antibody against the H,K-ATPase β subunit was kindly provided by J. Forte and D. Chow; University of California at Berkeley, Berkeley CA) diluted 1:10 in PBS⁺⁺ (PBS, 0.1 mM CaCl₂, 1 mM MgCl₂) + 0.1% BSA for 4–5 h. Nonspecific Ab binding was removed in three consecutive 10 min washes in PBS⁺⁺ + 0.1% BSA. Cells were fixed in cold methanol (–20 °C) for 10 min, followed by permeabilization and incubation with a goat anti-mouse rhodamine-conjugated secondary antibody (Sigma) as described previously (21).

Permeabilized Cells—Indirect immunofluorescence was conducted as described previously (21). Briefly, cells were fixed in 3.5% paraformaldehyde and permeabilized in 0.3% Triton X-100 before incubation in 1:500 rat monoclonal FcR2-B2 antibody (6B7B, gift of I. Mellman). Confocal images were generated using a Zeiss LSM 410 laser-scanning confocal microscope. All images were line averaged 8-fold. Cross-sections were generated with a 0.2 μ motor step. Contrast and brightness settings were adjusted so that all pixels were in the linear range.

Immunoelectron Microscopy

Cells grown on Transwell filters (Corning Costar) were rinsed twice in PBS⁺⁺ and fixed in 3% paraformaldehyde, 0.05% glutaraldehyde for 1 h at room temperature. Cells were labeled with anti-HA antibody, followed by goat anti-rabbit IgG conjugated to horseradish peroxidase (Biosys). Filters were labeled with peroxidase, embedded, and sectioned according to standard protocol (26).

Biotinylation

MDCK cells expressing H,K-ATPase β or the H,K/Na,K-ATPase β chimeras were grown to confluency on Transwell filters (Corning Costar). The filters were biotinylated at pH 7.5 from either the apical or basolateral membrane at 4 °C as described previously (27). Biotin was quenched with the addition of 100 mM glycine and the cells were lysed in 1 ml of 1% Triton X-100, 150 mM NaCl, 5 mM EDTA, 50 mM Tris, pH 7.5. One-eighth of the total lysate was then immunoprecipitated with 100 μ l of a 50/50 slurry of avidin-agarose. The biotinylated proteins were eluted from the beads by heating to 80 °C in SDS-PAGE sample buffer and separated on 10% polyacrylamide gels (28), transferred to nitrocellulose (29), and probed for 1 h at room temperature with 1:500 HK β antibody diluted into TBS (20 mM Tris-HCl, pH 7.5, 150 mM NaCl, 0.1% Tween 20) plus 5% powdered milk. The blot was then washed for 1 h in TBS + milk, and incubated with 1:1000 horseradish peroxidase-conjugated goat anti-mouse secondary antibody. Following further washes in TBS, the blot was developed with enhanced chemiluminescence (Amersham Pharmacia Biotech) and exposed to Hyperfilm (Amersham).

Internalization Assay

Measurements of HA-Y543 endocytosis were performed according to Brewer and Roth (12). Briefly, HA-Y543-expressing cells grown to confluency on Transwell filters were incubated at 37 °C for 40 min in Met-Cys-free medium and labeled for 30 min with ³⁵S-Met and Cys (ICN Radiochemicals, Irving, CA). Cells were chased with complete

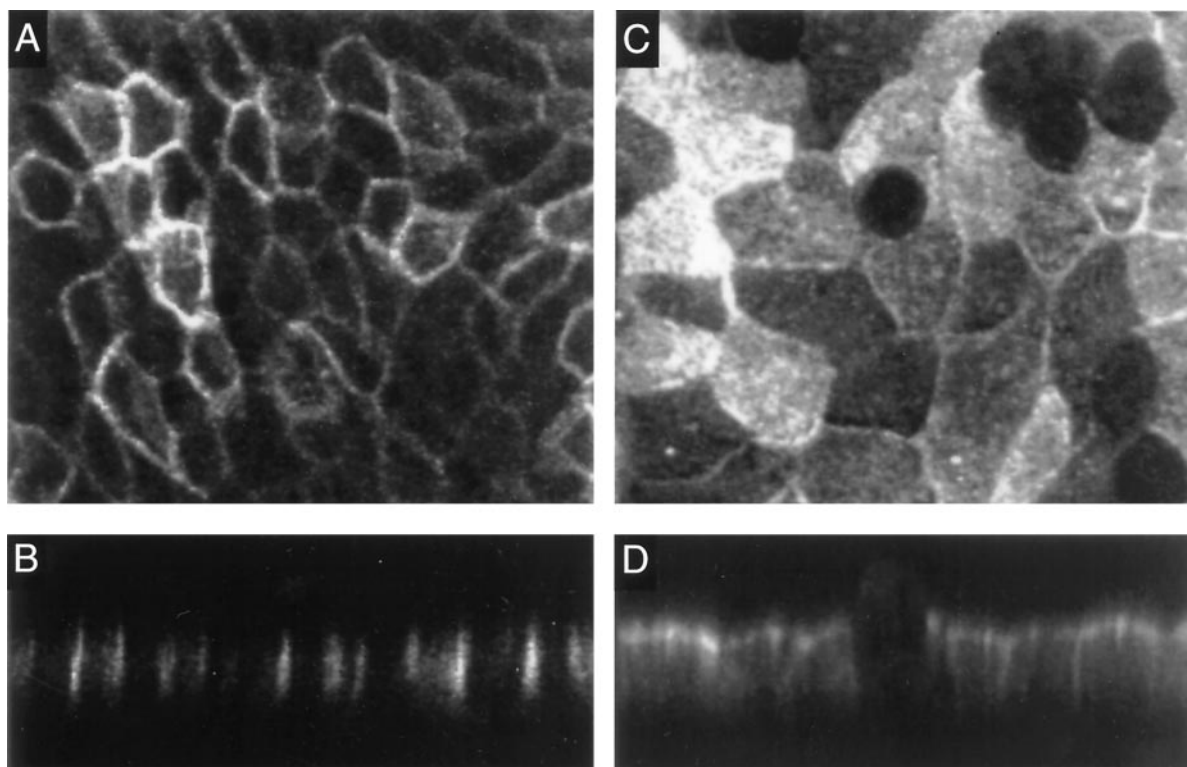


FIG. 1. **Steady state localization of the H,K-ATPase β subunit in MDCK and LLC-PK₁ cells.** Stably transfected cells grown on polycarbonate filters were incubated with a primary antibody against the ectodomain of the H,K-ATPase β subunit at 4 °C for 4 h. Cells were then washed, fixed in methanol (−20 °C) and incubated with a goat anti-mouse rhodamine-conjugated secondary antibody. Confocal images were collected on a Zeiss laser scanning confocal microscope. H,K-ATPase β is restricted to the basolateral domain of MDCK cells, both en face (A) and in X/Z cross-section (B). This protein is predominately localized to the apical domain in LLC-PK₁ cells, both en face (C) and in X/Z cross-section (D).

medium for 2 h at 37 °C. The medium was then replaced with ice-cold medium, and the cells were transferred to 4 °C. Anti-HA antibody was added to the medium in either the apical or the basolateral compartment, and the filters were incubated on ice for an additional 40 min. Filters were then washed twice in low HCO₃ DMEM containing 10 mM Hepes and 0.5% BSA and once in DMEM, 10 mM Hepes. Warmed (37 °C) DMEM, 10 mM Hepes was placed on the filters, which were moved to a 37 °C water bath for 1 min and then returned to 4 °C. Compartments previously containing antibody were treated with 100 μ g/ml trypsin for 40 min; soybean trypsin inhibitor (200 μ g/ml) was added to the opposite compartment. HA still remaining on the surface was cleaved into two fragments. Filters were rinsed in medium containing 200 μ g/ml soybean trypsin inhibitor for 10 min, 4 °C, and the cells were lysed in 50 mM Tris-HCl, pH 8.0, 10 mM EDTA, 1% Nonidet P-40, 0.1% SDS, 0.1 units of aprotinin. HA-Y543 was recovered by immunoprecipitation with protein A-agarose, separated by SDS-PAGE (28) and detected by fluorography using Autofluor (National Diagnostics, Manville, NJ). Band intensity was determined by densitometry. Percent internalized was calculated as uncleaved HA divided by total (uncleaved plus cleaved) HA.

RESULTS

MDCK cells were stably transfected with the rabbit gastric H,K-ATPase β subunit cDNA. Steady state localization of the H,K-ATPase β subunit polypeptide was determined by surface immunofluorescence, employing a monoclonal antibody directed against the ectodomain of the β subunit. Stably transfected MDCK cells were grown as confluent monolayers on polycarbonate filters and incubated at 4 °C for 4 h with monoclonal Ab present in both the apical and basolateral chambers. The monolayers were fixed and stained with a goat anti-mouse rhodamine-conjugated secondary Ab. Fluorescent images, both en face and in X/Z cross-section, were gathered with a laser-scanning confocal microscope. As can be seen in Fig. 1, A and B, the steady state distribution of the H,K-ATPase β subunit is restricted to the basolateral membrane. Cell surface biotinylation was also performed on transfected MDCK monolayers

grown on filters. These studies verify that the H,K-ATPase β subunit is localized 94 \pm 4% to the basolateral membrane domain (Fig. 5, A and B). Immunoprecipitation experiments indicate that, when expressed in mammalian cells, the H,K-ATPase β subunit does not form a stable complex with the endogenous Na,K-ATPase α subunit (data not shown). The H,K-ATPase β subunit basolateral localization is consistent therefore, with the possibility that this protein contains a signal that is interpreted as a basolateral sorting determinant in MDCK cells. Interestingly, when this protein is examined in another cell line derived from mammalian kidney, LLC-PK₁, it maintains a very different steady state distribution. In stably transfected LLC-PK₁ cells, surface immunofluorescence reveals that the H,K-ATPase β subunit is localized predominantly to the apical plasma membrane (Fig. 1, C and D).

To determine whether this differential sorting behavior was unique to the H,K-ATPase β subunit, or extended to other proteins bearing tyrosine-dependent sequence motifs, HA-Y543 was stably expressed in LLC-PK₁ cells. Wild type influenza HA protein is targeted to the apical membrane domains of both MDCK (30, 31) and LLC-PK₁ cells (Fig. 2A). Mutation of HA Cys-543 to a tyrosine creates an overlapping sorting and internalization sequence that directs the polypeptide to the basolateral membrane of MDCK cells (12). Immunoperoxidase-stained electron micrographs of LLC-PK₁ cells stably expressing either the wild type HA protein or HA-Y543 are depicted in Fig. 2, A and B. HA-Y543 is predominately intracellular, consistent with its steady state distribution in MDCK cells (12). HA-Y543 is localized to the apical domain (Fig. 2B) when surface staining is detected in cells selected for low level expression. Polarized distribution is lost when HA-Y543 is expressed at high levels (data not shown). Recent work demonstrates that the tyrosine-motif in HA-Y543 (YRIC) constitutes

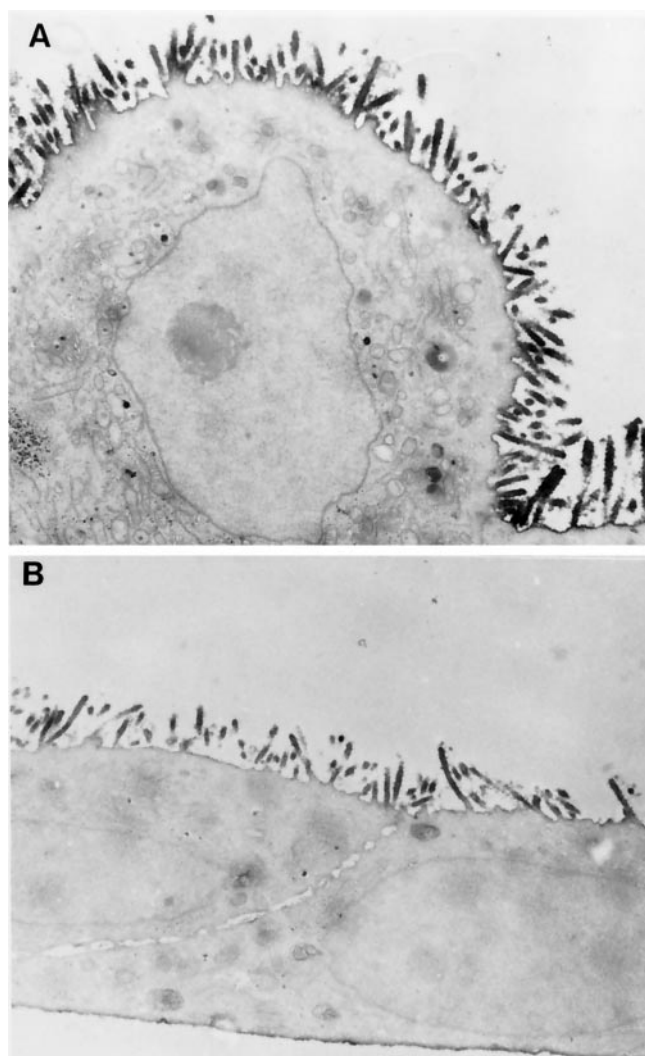


FIG. 2. Immunolocalization of influenza HA and HA-Y543 in LLC-PK₁ cells. HA or HA-Y543 stably expressed in LLC-PK₁ cells was analyzed by immunoelectron microscopy employing an ectodomain HA antibody and a goat anti-rabbit horseradish peroxidase conjugated secondary antibody. Dense horseradish peroxidase reaction product was localized to the apical brush border of cells expressing the wild type HA (A) protein. Horseradish peroxidase reaction product was also localized to the apical brush border and to a population of intracellular vesicles in cells expressing the HA-Y543 protein (B). No reaction product was detectable at the basolateral membranes of cells expressing low levels of either protein. Magnification, $\times 10,000$.

a relatively weak signal, which accounts for the loss of polarity at high levels of expression (32).³

The observations that the same proteins were sorted to distinct domains in cell lines resembling different nephron segments might reflect functional differences in the apical membranes of those cell types. Many tyrosine-based motifs contain overlapping information for intracellular sorting and for internalization from the plasma membrane (9–11). Localization of proteins containing these motifs to the opposite surfaces in MDCK and LLC-PK₁ cells may reflect different capacities for endocytosis at these membrane domains in the two cell types. To test this hypothesis, the relative apical and basolateral rates of endocytosis of HA-Y543 were determined in the MDCK and LLC-PK₁ cells. Cells grown on polycarbonate filters were labeled with ³⁵S-Met and Cys and chased for 2 h. The cells were then cooled to 4 °C and anti-HA antibody added to either the

TABLE I
Internalization of HA-Y543 in MDCK and LLC-PK₁ cells
Values are the percent of HA-Y543 present at the designated surface domain internalized after 1 min.

Cell type	Apical	Basolateral
MDCK	1.3 \pm 0.3	8.8 \pm 0.6 n = 3
LLC-PK ₁	7.0 \pm 0.6	17.1 \pm 1.1 n = 3

apical or the basolateral medium. After warming the filters to 37 °C for 1 min, surface bound Ab was removed by the addition of trypsin to the medium compartments. Internalized HA-Y543 was immunoprecipitated and the resulting SDS-PAGE bands quantified. In MDCK cells, apical endocytosis occurs at only 14% of the rate of basolateral endocytosis (Table I). However, in LLC-PK₁ cells, the apical surface is considerably more endocytically active, with internalization occurring at 41% of the basolateral rate (Table I).

To determine whether the tyrosine-dependent sequence motifs play a role in sorting to the different membrane domains of the MDCK and LLC-PK₁ cell lines, a chimera between the H,K-ATPase and the Na,K-ATPase β subunits was created. The Na,K-ATPase β subunit does not contain an equivalent tyrosine-based motif. The β N28H chimera replaces the cytoplasmic tail of the H,K-ATPase β subunit, excluding the three amino acids immediately adjacent to the transmembrane domain, with the cytoplasmic tail of the Na,K-ATPase β subunit. The β H-Y20A construct mutates Tyr-20 to an alanine. Similar point mutations in other proteins have been shown to significantly reduce the capacity of this motif for internalization (33, 34). This mutation also disrupts internalization of the functional gastric H,K-ATPase holoenzyme from the surfaces of gastric parietal cells *in vivo* when it is expressed in transgenic mice (35). The constructs are depicted in Fig. 3.

These constructs were stably transfected into the MDCK and LLC-PK₁ cell lines and their steady state distributions determined as described for the wild type H,K-ATPase β subunit. In MDCK cells, significant fractions of both the β N28H and β H-Y20A chimeras were localized at steady state to the apical membrane domain (Fig. 4, A–D). This observation supports our hypothesis that sorting information is contained within the cytoplasmic tail and, more specifically, within the tyrosine-based sorting motif of the H,K-ATPase β subunit. Cell surface biotinylation confirms the steady state localization of the β subunit chimeras to both the apical and basolateral membrane domains of MDCK cells (Fig. 5, A and B). Densitometric quantitation of these data (Fig. 5B) verify that the localization of β N28H is 31 \pm 7% apical, whereas that of β H-Y20A is 42 \pm 2% apical. In contrast, 6 \pm 4% of the wild type H,K-ATPase β subunit is apically localized.

Both surface immunofluorescence and biotinylation represent powerful tools to determine protein distribution in MDCK cells. These methods introduce the minimum of cell type specific artifact, as the respective reagents used for detection have access to the “unmanipulated” localization of the β subunit chimeras before either fixation or cell lysis and immunoprecipitation. The data presented in Figs. 1, 4, and 5 strongly confirm the localization of the H,K-ATPase β subunit to the basolateral membrane of MDCK cells, and the localization of the β subunit chimeras to both the apical and basolateral membranes of MDCK cells. Surface immunofluorescence remains applicable in LLC-PK₁ cells. However, the presence of a dense glycocalyx in these cells hinders access to the apical membrane and renders biotinylation a less definitive means for protein localization in LLC-PK₁ cells (27).

Confocal microscopy revealed that in the stably transfected LLC-PK₁ cell lines, all of the β subunit chimeras retained a

³ H. Y. Naim and M. G. Roth, unpublished observations.

H,K-ATPase β : NH₂-MAALQEKKKSCSRMEEFRHYCWNPDTGQMLGRILSR- TM
 Na,K-ATPase β -NH₂-**MARGKAKEEGSWKKFIWDESEKKEFLGRGTGS**- TM
 β N28H NH₂-**MARGKAKEEGSWKKFIWDESEKKEFLGRILSR**- TM
 β H-Y20 NH₂-MAALQEKKKSCSRMEEFRHACWNPDTGQMLGRILSR- TM

FIG. 3. **Constructs incorporating portions of the H,K-ATPase β and the highly homologous Na,K-ATPase β are depicted schematically.** Na,K-ATPase β sequence is shown in *bold type*, the mutated sequence is *underlined* and *bold*. β N28H replaces all but the three most membrane-proximal amino acids of the H,K-ATPase β cytoplasmic tail with the Na,K-ATPase β cytoplasmic tail. β H-Y20A mutates tyrosine-20 of the tyrosine-dependent motif to an alanine.

predominately apical steady state distribution, similar to that found for the wild type H,K-ATPase β subunit (Fig. 6, A–D). The FRHY motif does not, therefore, seem to be required for sorting to the endocytically active apical domain of LLC-PK₁ cells. Furthermore, the observation that β N28H remains localized predominately to the apical membrane (Fig. 6, A and B) indicates that the entire cytoplasmic tail of the H,K-ATPase β subunit does not seem to play a dominant role in the sorting behavior of this protein in the LLC-PK₁ cell line.

The FcR2-B2 protein relies upon a tyrosine-independent di-leucine motif for internalization and for basolateral sorting in MDCK cells (18, 19, 24). Both en face (Fig. 7A) and XZ cross section (Fig. 7B) confocal images of indirect immunofluorescence indicate that this protein remains basolaterally localized when stably expressed in LLC-PK₁ cells. Cell surface biotinylation is consistent with the immunocytochemical results, verifying that the FcR2-B2 protein accumulates at the basolateral domain in LLC-PK₁ cells, as it does in the MDCK cell line (data not shown). These data suggest that the sorting and internalization motifs are, as a class, differentially interpreted in the MDCK and LLC-PK₁ cell lines.

DISCUSSION

Previous studies have indicated that diverse epithelial cells have the ability to sort similar proteins to distinct surface distributions. For example, in MDCK cells glycosylphosphatidylinositol-linked proteins are sorted to the apical membrane (36, 37), whereas members of this family are directed to the basolateral domain in Fisher rat thyroid epithelial cells (38). Additionally, the Na,K-ATPase ion pump resides in the basolateral membrane of most epithelial cells, but is localized to the apical membrane domain in cells of the choroid plexus (39) and the retinal pigment epithelium (40). It would appear, therefore, that sorting mechanisms vary among cell types. This variability may provide different epithelial cell types with the flexibility to establish domains that contain distinct proteins in response to particular physiological requirements.

We have demonstrated that the H,K-ATPase β subunit cytoplasmic tail contains one class of recognized sorting sequence, a tyrosine-dependent motif, which is interpreted as a basolateral sorting determinant in MDCK cells. LLC-PK₁ cells, however, accumulate proteins containing tyrosine-dependent motifs at the apical membrane domain. Interestingly, alteration of this motif affects the sorting behavior of the H,K-ATPase β subunit in MDCK cells, whereas the sorting behavior of this protein remains unchanged in LLC-PK₁ cells. Two polarized renal epithelial cell lines can, therefore, respond differently to the sorting information contained in a single, narrowly defined, amino acid sequence.

Disruption of the tyrosine motif in the H,K-ATPase β subunit markedly alters the distribution of this subunit in MDCK cells (Figs. 4 and 5). Although only 6% of the wild type protein is found at the apical surface, 42% of β H-Y20A and 31% of β N28H are detected at the apical plasmalemma. The values obtained

for β H-Y20A and β N28H are comparable with those derived from measurements of the fraction of the plasma membrane surface area associated with the apical domain in MDCK cells grown on filters (41). Thus, these results are consistent with the possibility that the default pathway for membrane proteins in MDCK cells leads to accumulation in both the apical and the basolateral membrane domains. Further support for this conclusion is derived from recent studies of γ -aminobutyric acid transporter constructs (42), the CD7 receptor (43), and the transferrin receptor (44) in MDCK cells. Additionally, these results imply that proteins that accumulate predominately at the apical surface upon disruption of known basolateral motifs may contain previously unrecognized apical sorting information. Such behavior has been noted for the LDL receptor (13) and pIGR (8). Finally, disruption of known secreted protein sorting signals (45), or of the mechanisms of secreted protein sorting (46), leads to apolar protein secretion. The default pathway for membrane proteins thus appears parallel to the well established default pathway for secreted proteins in MDCK cells.

N-Glycosylation has been implicated as a potentially important determinant for sorting to the apical membrane domain of MDCK cells (47). In this context, it is interesting to note that apically biotinylated H,K-ATPase β , β H-Y20A and to a lesser degree, β N28H, all possess slightly higher apparent molecular weights than the population of protein biotinylated from the basolateral surface (Fig. 5A). Treatment of these biotinylated and immunoprecipitated protein populations with endoglycosidase F or with neuraminidase reduces the isolated proteins to similar molecular weights (data not shown). It would appear, therefore, that apical protein populations are hypersialylated in comparison to basolateral protein populations. However, pulse-chase experiments indicate that both the H,K-ATPase β subunit and β H-Y20A are initially delivered to the cell surface with similar molecular weights (data not shown). N-Glycosylation and sialylation of the H,K-ATPase β subunit does not, therefore, appear to contribute any apical sorting information, or to play a role in the initial sorting of these proteins. Instead, events subsequent to arrival at the cell surface produce the observed dissimilarity in glycosylation state.

The precise cells within the mammalian kidney from which the MDCK and LLC-PK₁ cell lines are derived are unknown. It has been noted, however, that LLC-PK₁ cells morphologically and functionally resemble cells found in the proximal tubule of the nephron (48), whereas MDCK cells resemble those found in the distal nephron segments (49). Perfusion studies using fluorescein isothiocyanate dextran have shown that proximal tubule cells endocytose marker from their apical surfaces, whereas only intercalated and ADH-stimulated principal cells from the collecting duct endocytose marker from their apical membrane (50). In addition, a significantly larger percent of HA-Y543 is internalized from the apical membrane domain of LLC-PK₁ cells than from the apical membrane domain of MDCK cells (Table I). Because both LLC-PK₁ cells (48) and MDCK cells grown on polycarbonate filters (41) can attain close to 1:1 apical to basolateral membrane surface areas, this reflects an increase in the endocytic capacity at the LLC-PK₁ apical membrane. Conceivably, the differential localizations of the proteins examined in this work could be attributable to the varying physiological properties of the nephron segments these cells resemble. According to this hypothesis, proteins exhibiting overlapping sorting and internalization motifs are directed to a cell's most endocytically active domain. It must be noted, however, that the β subunit chimeras lacking tyrosine-dependent sorting motifs are found at the apical surface in LLC-PK₁ cells (Fig. 6). This interpretation, therefore, appears unlikely to

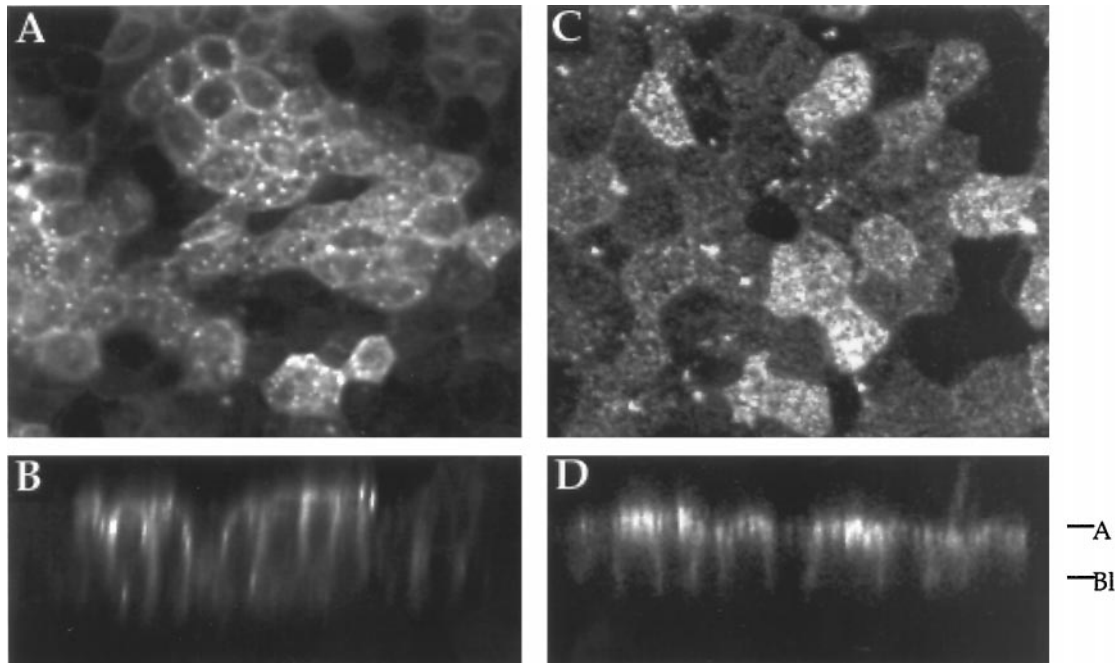


FIG. 4. **Steady state localization of the H,K/Na,K-ATPase β constructs in MDCK cells.** The steady state localization of the H,K/Na,K-ATPase β chimeras in stably transfected MDCK cells was examined by surface immunofluorescence. En face (A and C) and X/Z cross-section (B and D) confocal images indicate significant apical localization of β N28H (A and B), β H-Y20A (C and D).

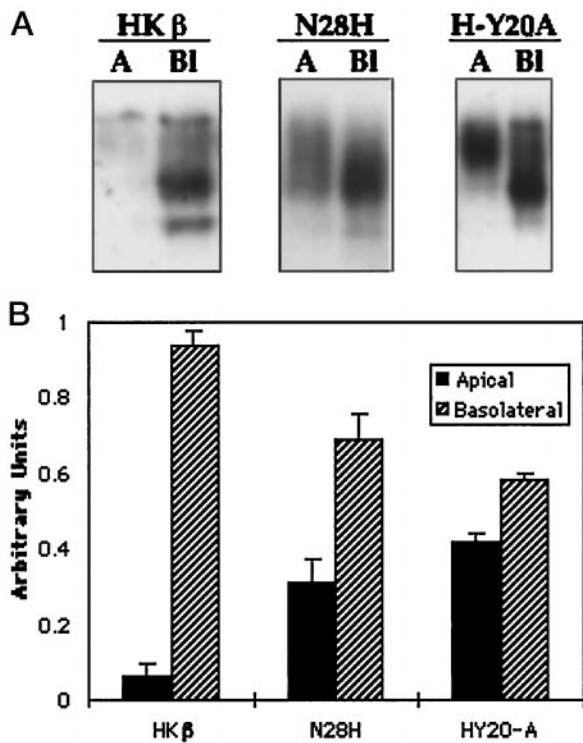


FIG. 5. **Biotinylation of the H,K/Na,K-ATPase β constructs in MDCK cells.** Stably transfected cells were grown on polycarbonate filters and biotinylated from either the apical (A) or the basolateral (BI) domain at pH 7.5. Biotinylated proteins were recovered by immunoprecipitation on streptavidin-agarose beads and analyzed by Western blot. Mature H,K β , β N28H and β HY-20A all run as heavily glycosylated bands between 50–60 kDa. Although H,K β is restricted to the basolateral membrane, significant populations of β N28H and β H-Y20A are accessible from the apical membrane (panel A). Four experiments for each construct were quantitated using the IS-1000 Digital Imaging system (Alpha Innotech Corp., San Leandro, CA) (panel B). Solid black bars, percentage of apically localized protein; hatched bars, percentage of basolaterally localized protein. Error bars depict the S.E.

be correct. The differential distribution of these proteins does not appear to be attributable to domain specific differences in endocytic capacity between these polarized cell types.

The apical localization of proteins with tyrosine-dependent motifs in LLC-PK₁ cells does not, however, appear to be attributable to divergent behavior of a tissue culture cell line. Recent studies examined the localization of the LDL receptor expressed under the control of the metallothionein promoter in transgenic mice (51). The LDL receptor contains two tyrosine-dependent basolateral sorting motifs, one of which overlaps an internalization signal. This receptor accumulates at the basolateral membrane when stably expressed in MDCK cells (13). In contrast, when expressed in the kidney of transgenic mice, this receptor is localized to the apical domain of proximal tubule cells (51).

The observations in this report suggest a mechanism by which plasticity in sorting classes of membrane proteins in epithelial cells could be achieved. As β subunit constructs lacking tyrosine-dependent sorting motifs were found at the apical surface of LLC-PK₁ cells (Fig. 6), these motifs did not function directly as apical sorting signals in these cells, and the β subunit must contain other features that allow it to be sorted apically. The fact that tyrosine-dependent motifs in both the β subunit and in HA-Y543 failed to specify basolateral sorting in LLC-PK₁ cells indicates that this cell type has diminished capacity to recognize this class of basolateral signal. As a result, cryptic apical sorting information in the β subunit and in the HA-Y543 protein becomes dominant, allowing both proteins to be sorted apically. In contrast, the FcRII-B2, which relies upon a di-leucine motif for basolateral sorting, was located basolaterally in LLC-PK₁ cells (Fig. 7). As the FcRII-B2 is sorted apically in MDCK cells when its cytoplasmic basolateral sorting signal is removed (11, 20), this protein also appears to contain cryptic apical sorting information. It is likely, therefore, that the basolateral sorting of FcRII-B2 observed in LLC-PK₁ cells is attributable to the dominant basolateral sorting signal contributed by the di-leucine motif. Taken together, these observations indicate that the cellular mechanisms responsible for recognizing di-leucine motifs and tyrosine-

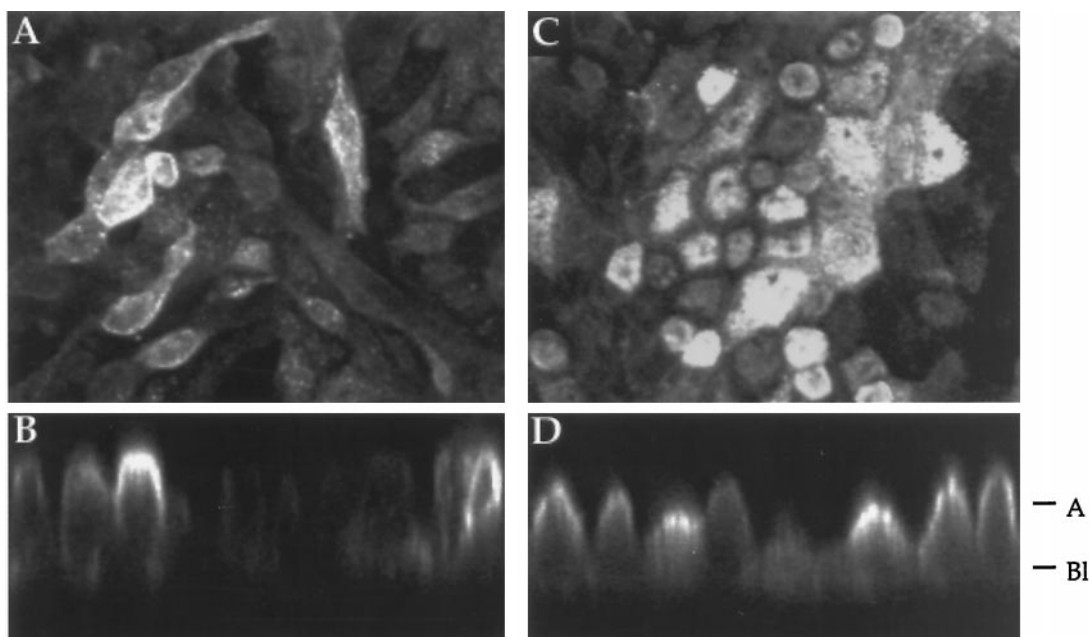


FIG. 6. **Steady state localization of the H,K/Na,K-ATPase constructs in LLC-PK₁ cells.** The steady state localization of the H,K/Na,K-ATPase β constructs in stably transfected LLC-PK₁ cells was examined by surface immunofluorescence. En face (A and C) and X/Z cross-section (B and D) confocal images indicate a predominately apical localization of β N28H (A and B), β H-Y20A (C and D).

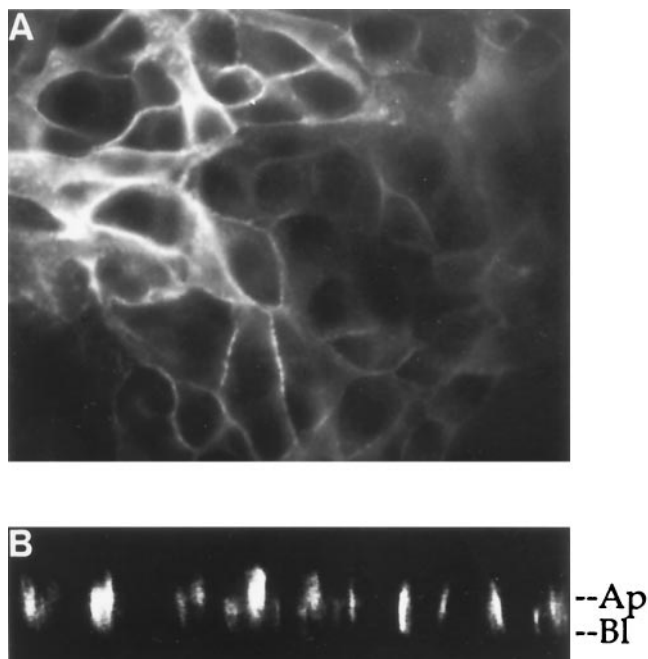


FIG. 7. **Localization of FcRII-B2 in LLC-PK₁ Cells.** Steady state localization of the FcRII-B2 protein in stably expressing LLC-PK₁ cells was determined by indirect immunofluorescence. Following fixation in methanol, cells grown on polycarbonate filters were incubated with a primary antibody directed against the FcRII-B2 protein and an anti-mouse rhodamine-conjugated secondary antibody. En face (A) and X/Z cross-section (B) confocal images reveal that the FcRII-B2 protein is restricted to the basolateral domain.

dependent motifs are distinct and can be regulated with varying intensities. This conclusion is consistent with data from recent studies that demonstrated that di-leucine and tyrosine-based signals do not compete with one another for cell surface adaptor binding (52). It would appear that although different classes of signal can specify the same distribution or dynamic behavior, distinct components of the cellular sorting machinery are responsible for interpreting their messages. Our studies indicate that individual epithelial cell types may be able to

tailor the cell surface distributions of their membrane proteins to meet the requirements imposed by their physiologic functions. This plasticity appears to be achieved by altering the relative activities of the mechanisms that decode multiple sorting signals present in individual proteins.

Acknowledgments—We thank Drs. M. Rueben, G. Sachs, J. Forte, D. Chow, K. Matter, I. Mellman, L. Roman, K. Matlin, and K. Amsler for generously sharing reagents. Sue Anne Mentone provided excellent technical assistance in the preparation of the electron micrographs. We also thank Grazia Pietrini and the members of the Caplan Laboratory for helpful discussions and suggestions.

REFERENCES

- Rodriguez-Boulant, E., and Nelson, W. J. (1989) *Science* **245**, 718–725
- Matlin, K., and Caplan, M. J. (1992) in *The Kidney: Physiology and Pathophysiology, Second Edition* (Giebisch, G., and Seldin, D. W., eds), pp. 447–473, Raven Press, Ltd., New York
- Kundu, A., Avalos, R. T., Sanderson, C. M., and Nayak, D. P. (1996) *J. Virol.* **70**, 6508–6515
- Vogel, L. K., Noren, O., and Sjostrom, H. (1995) *J. Biol. Chem.* **270**, 22933–22938
- McQueen, N., Nayak, D., Stephens, E. B., and Compans, R. W. (1986) *Proc. Natl. Acad. Sci. U. S. A.* **83**, 9318–9322
- Roth, M. G., Gunderson, D., Patil, N., and Rodriguez-Boulant, E. J. (1987) *J. Cell Biol.* **104**, 769–782
- Mostov, K. E., Breitfeld, P., and Harris, J. M. (1987) *J. Cell Biol.* **105**, 2031–2036
- Casanova, J. E., Apodaca, G., and Mostov, K. E. (1991) *Cell* **66**, 65–75
- Geffen, I., Fuhrer, C., Leitinger, B., Weiss, M., Huggel, K., Griffiths, G., and Spiess, M. (1993) *J. Biol. Chem.* **268**, 20772–20777
- Prill, V., Lehmann, L., von Figura, K., and Peters, C. (1993) *EMBO J.* **12**, 2181–2193
- Hunziker, W., Harter, C., Matter, K., and Mellman, I. (1991) *Cell* **66**, 907–920
- Brewer, C. B., and Roth, M. G. (1991) *J. Cell Biol.* **114**, 413–421
- Matter, K., Hunziker, W., and Mellman, I. (1992) *Cell* **71**, 741–753
- Thomas, D., and Roth, M. G. (1994) *J. Biol. Chem.* **269**, 15732–15739
- Davis, C. G., van Driel, I. R., Russell, D. W., Brown, M. S., and Goldstein, J. L. (1987) *J. Biol. Chem.* **262**, 4075–4082
- Lazarovits, J., and Roth, M. G. (1988) *Cell* **53**, 743–752
- Collawn, J. F., Stangel, M., Kuhn, L. A., Esekogwu, V., Jing, S., Trowbridge, I. S., and Tainer, J. A. (1990) *Cell* **63**, 1061–1072
- Hunziker, W., and Mellman, I. (1989) *J. Cell Biol.* **109**, 3291–3302
- Matter, K., Yamamoto, E. M., and Mellman, I. (1994) *J. Cell Biol.* **126**, 991–1004
- Hunziker, W., and Fumey, C. (1994) *EMBO J.* **13**, 2963–2969
- Gottardi, C. J., and Caplan, M. J. (1993a) *J. Cell Biol.* **121**, 283–293
- Girones, N., Alvarez, E., Seth, A., Lin, I.-M., Latour, D. A., and Davis, R. J. (1991) *J. Biol. Chem.* **266**, 19006–19012
- Gottardi, C. J., and Caplan, M. J. (1993c) *J. Biol. Chem.* **268**, 14342–14347
- Miettinen, H., Matter, K., Hunziker, W., Rose, J., and Mellman, I. (1992) *J. Cell Biol.* **116**, 875–888
- Reuben, M. A., Lasater, L. S., and Sachs, G. (1990) *Proc. Natl. Acad. Sci.*

- U. S. A. **87**, 6767–6771
26. Machamer, C., Mentone, S., Rose, J. K., and Farquar, M. G. (1990) *Proc. Natl. Acad. Sci. U. S. A.* **87**, 6944–6948
27. Gottardi, C. J., Dunbar L. A., and Caplan, M. J. (1995) *Am. J. Physiol.* **268**, F285–F295
28. Laemmli, U. K. (1970) *Nature* **227**, 680–685
29. Towbin, H., Staehelin, T., and Gordon, J. (1979) *Proc. Natl. Acad. Sci. U. S. A.* **76**, 4350–4354
30. Rodriguez-Boulau, E., and Sabatini, D., D. (1978) *Proc. Natl. Acad. Sci. U. S. A.* **75**, 5071–5075
31. Stephans, E. B., Compans, R. W., Earl, P., and Moss, B. (1986) *EMBO J.* **5**, 237–245
32. Naim, H. Y., and Roth, M. G. (1994) *J. Biol. Chem.* **269**, 3928–3933
33. Alvarez, E., Girones, N., and Davis, R. J. (1993) *Biochem. J.* **267**, 31–35
34. Fuhrer, C., Geffen, I., and Spiess, M. (1991) *J. Cell Biol.* **114**, 423–431
35. Courtois-Coutry, N., Roush, D., Rajendran, V., McCarthy, J. B., Geibel, J., Kashgarian, M., and Caplan, M. J. (1997) *Cell* **90**, 501–510
36. Brown, D. A., Crise, B., and Rose, J. K. (1989) *Science* **245**, 1499–1501
37. Lisanti, M., Caras, I., Davitz, M., and Rodriguez-Boulau, E. (1989) *J. Cell Biol.* **109**, 2145–2156
38. Zurzolo, C., Lisanti, M. P., Caras, I. W., Nitsch, L., and Rodriguez-Boulau, E. (1993) *J. Cell Biol.* **121**, 1031–1039
39. Masuzawa, T., Ohta, T., Kawamura, M., Nakahara, N., and Sato, F. (1984) *Brain Res.* **302**, 357–362
40. Gundersen, D., Orłowski, J., and Rodriguez-Boulau, E. (1991) *J. Cell Biol.* **112**, 863–872
41. Butor, C., and Davoust, J. (1992) *Exp. Cell Res.* **203**, 115–127
42. Muth, T. R., Ahn, J., and Caplan, M. J. (1998) *J. Biol. Chem.* **273**, 25616–25627
43. Haller, C., and Alper, S. L. (1993) *Am. J. Physiol.* **265**, C1069–C1079
44. Odorizzi, G., Pearse, A., Domingo, D., Trowbridge, I. S., and Hopkins, C. R. (1996) *J. Cell Biol.* **135**, 139–152
45. De Strooper, B., Craessaerts, K., Van Leuven, F., and Van Den Berghe, H. (1995) *J. Biol. Chem.* **270**, 30310–30314
46. Caplan, M. J., Stow, J. L., Newman, A. P., Madri, J., Anderson, H. C., Farquhar, M. G., Palade, G. E., and Jamieson, J. D. (1987) *Nature* **329**, 632–635
47. Scheiffele, P., Peranen, J., and Simons, K. (1995) *Nature* **378**, 96–98
48. Pfaller, W., Gstraunthalerand, G., and Loidl, P. (1990) *J. Cell. Physiol.* **142**, 247–254
49. Herzlinger, D. A., Easton, T. G., and Ojakian, G. K. (1982) *J. Cell Biol.* **93**, 269–277
50. Schwartz, G., and Al-Awqati, Q. (1985) *J. Clin. Invest.* **75**, 1638–1644
51. Pathak, R. K., Yokode, M., Hammer, R. E., Hofmann, S. L., Brown, M. S., Goldstein, J. L., and Anderson, R. G. W. (1990) *J. Cell Biol.* **111**, 347–359
52. Marks, M. S., Woodruff, L., Ohno, H., and Bonifacino, J. S. (1996) *J. Cell Biol.* **135**, 341–354